A Low Mutual Coupling Antenna Array with Gain Enhancement Using Metamaterial Loading and Neutralization Line Structure

Shengyuan Luo [1], Yingsong Li [1,2,*], Yinfeng Xia [1], and Liang Zhang [3]

[1] College of Information and Communication Engineering
Harbin Engineering University, Harbin, Heilongjiang 150001, China
liyingsong@ieee.org

[2] Key Laboratory of Microwave Sensing, National Space Science Center
Chinese Academy of Sciences, Beijing 100190, China

[3] AnHui Province Key Laboratory of Simulation and Design for Electronic Information System, Hefei 230601, China

Abstract **─** A MIMO antenna array with high isolation and gain enhancement operating at 5.7 GHz is proposed by using a metamaterial and neutralization line for wireless local area network (WLAN) communication system. A suspended meta-surface consisted of periodic metamaterial cells is installed on the top of the MIMO antenna array to realize a gain enhancement, while the low correlation is implemented by using the neutralization line decoupling structure which is adopted on the feeding lines. The proposed MIMO array is modeled in the HFSS, and it is well analyzed, optimized, fabricated, and measured to discuss its performance. The obtained results demonstrate that the proposed MIMO antenna array can cover the upper WLAN band with a gain enhancement of 3dB and mutual decoupling of 30dB in the operating band with an efficiency of 68%.

Index Terms **─** Gain enhancement, MIMO antenna array, mutual decoupling, WLAN.

I. INTRODUCTION

The increment of the mobile terminal users has boosted the development of wireless communication technologies and systems, including the antennas. Especially for the next-generation communications which need multiple-input multiple-output (MIMO) antenna array to enhance the system performance, the MIMO antenna array requires not only high gain but also high isolation to satisfy the great demand of high communication quality with millions of users.

To improve the communication quality, MIMO technology is a good candidate to increase throughput of the system and to reduce the multi-path effects [1]. Moreover, the terminals of the modern portable communications become to be smaller and smaller. Since the space in these terminals are limited, the distance between the antenna array elements is only a fraction of the wavelength in the operating band, which may cause a strong mutual coupling between these array elements [2]. The mutual coupling will seriously degrade the radiation performance of the antenna array. Additionally, if the MIMO antenna array does not have a high gain, it will result in a great waste of energy. Thus, how to improve the gain and the isolation of a MIMO antenna array has become to be an urgent problem. After that, many methods have been proposed and investigated to provide a high isolation since antenna array has been widely applied in military and industry.

To enhance the gain of the MIMO antenna array, numerous methods have been reported. The existing gain enhancement technologies include using reflectors, slotted metal wall, LTCC with a cavity inside the substrate, shorting pins, UC-EBG and near-zero refractive index metamaterial [3-12]. It is pointed out in [3] that both the gain and the frequency bandwidth of the antenna array have been improved simultaneously. In [4], the antenna array with several directors and a truncated ground plane acting as a reflector has been presented to maximize the antenna gain. Unlike the structure described in [4], a gain-enhanced circularly polarized antenna array is proposed by adding a slotted metal wall in [5]. In addition, low temperature co-fired ceramic (LTCC), as a multilayered technology, has been widely used in planner antenna design [6]. However, the radiation efficiency is severely reduced when the surface-wave power is increased in the antenna. Therefore, to maximize the radiation efficiency and antenna gain, low permittivity substrate is preferred and used for designing antenna arrays. But, the substrates with low permittivity are not currently available in LTCC technology. Thus, the cavity technology is used to improve the efficiency in [6-8]. Also, the LTCC technology is used to improve the antenna performance with low dielectric loss and low conductor losses while the fabrication cost is high. In [9],

Submitted On: November 10, 2018
Accepted On: December 1, 2018

a gain enhancement for a broadband symmetrical dual-loop antenna is presented, where a pair of shorting pins is symmetrically loaded beneath the radiator. Therefore, surface current crossing the center of the antenna can be significantly enhanced to improve its radiation directivity and gain. However, the increment in gain is not very high. The uniplanar-compact electro-magnetic band-gap (UC-EBG), referred in [10], is also an effective method to strengthen the gain of the antenna, where the antenna uses the periodic UC-EBG wrapped around the patch or placed under the radiation patch to implement as a reflector so that more energy is radiated toward a fixed direction. However, it needs more space to construct such a large reflector. Recently, the near zero refractive index metamaterial have been used and installed on the top of the patch antennas for achieving high gain [11-12].

On the other hand, the mutual coupling in the antenna array will also reduce the efficiency and peak gain. Thus, it is necessary to design a mutual decoupling structure to suppress the mutual coupling. In the past decades, many methods have been investigated for reducing the mutual decoupling between the antenna elements, and they have been proved to be effective, including spatial orthogonal current techniques, defected ground structure (DGS), electromagnetic band-gap (EBG), metamaterial and mutual decoupling networks [13-23]. The DGS has been developed to enhance the isolation between antenna array elements while it may destroy the integrity of the ground plane that may leak electromagnetic wave and deteriorate the radiation patterns [16-17]. Another effective method to reduce the mutual coupling of antenna array is implemented by loading the EBG structure between antenna array elements. The EBG can suppress the propagation of surface wave between array elements due to its high impendence property in the antenna operation frequency band. However, it can only reject the spread of surface waves rather than spatial waves [18-20]. Unlike EBG structure that requires shorting pins, metamaterial has been inserted between the antenna array elements, which is not suitable for the feed network design in massive antenna arrays [21-23]. For the mutual decoupling network referred in [24-25], it was only applied in mutual decoupling design of two-element antenna arrays.

Recently, the antenna array in base station needs a higher gain and isolation to serve dozens of mobile terminal users with more antenna elements over the upper WLAN work band. The mutual decoupling network has two features, the first feature is that it can be applied in mutual decoupling of massive MIMO antenna array with the feed network together, and the second feature is that it cannot only suppress the surface wave between MIMO array elements but also can prohibit the spatial waves over the patch. The metamaterial superstrate structure (MSS) has received growing interest because of its potential advantages in wireless communication technology, including the characteristics of easily design and simply fabrication. An MSS consists of metamaterial cells which are installed on the top of the antenna array to form a Fabry-Perot cavity for gain enhancement. In this paper, a closely installed MIMO antenna array is considered rather than a standard antenna array. We aim to reduce the mutual coupling and enhance the gain in comparison with the MIMO array without the decoupling structure and MSS loading. In the design, the distance between the array elements is 2mm and the edge-to-edge distance between the two arrays is 5mm. According to the advantages of the MSS and mutual decoupling network, a high isolation MIMO antenna array with gain enhancement is proposed by using MSS and mutual decoupling network operating at upper WLAN band. Comparing with the existing technology of MIMO antenna array, the MIMO antenna array proposed in this paper has the following unique features:

(1) The reported MIMO antenna array has a high gain and high isolation simultaneously.

(2) The mutual decoupling network can be adjusted to match with the original MIMO antenna array for effectively reducing the coupling at the operating band.

(3) The feed network and radiating patch are respectively located on both sides of the ground plane.

II. DESIGN OF THE PROPOSED MIMO ARRAY

A. Design of the MSS

The metamaterial is a favorable candidate for gain enhancement by properly adjusting its parameters, and it is also an artistic work to design a MSS which has a near zero refractive index property at the working frequency of four-element MIMO antenna array. The schematic of an MSS comes from the resonance of the inductance in the metal patch and the capacitance from the slots, which is shown in Fig. 1. Figure 1 (a) is the simulation model of the proposed MSS cell that is modified from a traditional split resonant ring (SRR). The boundaries are set to be PMC and PEC walls. The equivalent circuit of the design MSS cell is shown in Fig. 1 (a) at same time to illustrate the working mechanism of the metamaterial. To get the characteristics of the proposed MSS cell, the permittivity and permeability of the MSS are calculated and the results are shown in Fig. 1 (b). According to the metamaterial theory, Fabry-Perot cavity theory and the conventional cavity resonance condition, the dimensions of the metamaterial can be obtained. The conventional resonance cavity condition can be expressed as follow:

$$H + h1\sqrt{\varepsilon_r} = (\phi_{MS} + \phi_G)\frac{\lambda}{4\pi} \pm N\frac{\lambda}{2}, \qquad (1)$$

where ϕ_{MS} is the reflected wave phase of the MSS, ϕ_G is the reflected wave phase of the metal ground plane. H is the distance between ground metal and the upper surface of the coating metamaterial. The “N” is any integer value. When the parameter H is properly adjusted, a resonance cavity will be formed, where the electromagnetic waves will be reflected multiple times between metal ground plane and MSS. If the designed antenna meets the conventional resonance cavity condition, the reflected waves will pass through the MSS loading with same phase, which can strengthen the directionality of the MIMO antenna array, and the gain will be improved. The parameter has an important effect on the performance of the proposed MSS, and the reflected phase of the metamaterial cell with different a1 is shown in detail in Fig. 1 (c). It is observed that the phase of the operating frequency shifts to lower frequency as the parameter a1 increases from 3.5mm to 5.5mm.

B. High gain four –element antenna array design

The configuration of the proposed four-element MIMO antenna array without MSS is well designed and described in Fig. 2 (a). Aiming to compact the size and reduce the weight of the array, the proposed antenna array is realized based on the light weight and low profile microstrip antenna. The proposed antenna array has four microstrip patch antennas printed on the top of the FR4 substrate with a relative permittivity of 4.4 and a loss tangent of 0.02. A metal ground plane is placed on the bottom of the substrate. Because the distance of the inner-element is a small fraction of the wavelength, therefore, there is no enough space to locate a feed network. In this design, the feeding network is loaded on the bottom of the second substrate that is placed under the metal ground plane. The ground plane can reduce the interaction between feed network and antenna array. The antenna array and feed network are connected by metal probes to excite the antenna elements, which have some small holes on the metal ground plane. There is no gap between two substrates. It is to say that the MIMO antenna elements are designed on the top of the first substrate and the feeding network is printed on the bottom of the second substrate, while a common plane between the two substrates. The simulated S-parameters and radiation patterns of the original MIMO antenna array are described in Fig. 2 (b) and Fig. 2 (c), respectively. It can be found that the original MIMO antenna array has good impedance bandwidth ranging from 5.4-5.96 GHz, but the correlation coefficient between antenna array elements is high which might deteriorate the performance of the MIMO array. In this case, the gain of the antenna array is 5.3 dBi.

In previous engineering design of antenna array, the distance between the antenna array elements is half of the wavelength in substrate. But, when the four-element transmitting and receiving antenna are placed on the same substrate, the size of the antenna array is too large that cannot be easily integrated into a space-limited communication system. Therefore, it is an effective way to design an antenna array that can be integrated with mobile terminal by reducing the distance between antenna array elements. Comparing with the normal antenna array, the gain of compact array antenna maybe seriously deteriorated, and therefore, the gain enhancement operation should be developed to improve the radiation characteristics of the antenna array.

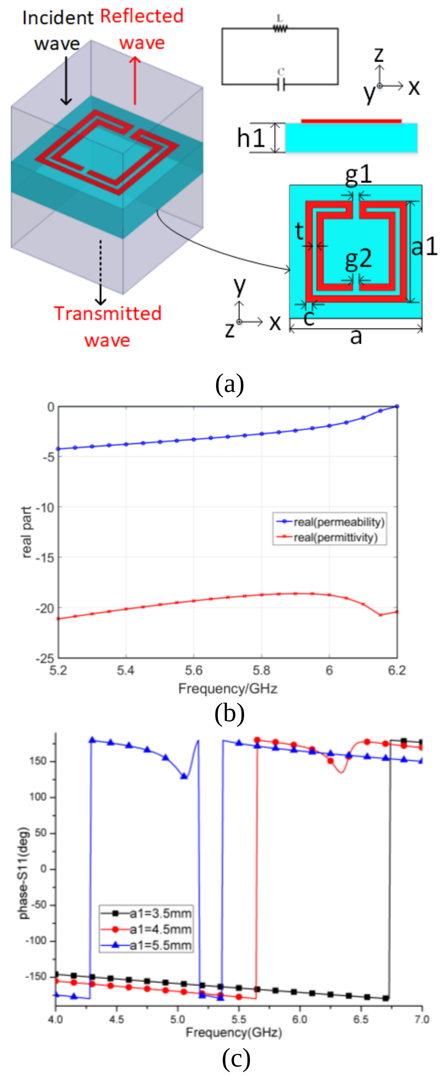

Fig. 1. (a) The electromagnetic simulation model of metamaterial cell, (b) the permittivity and permeability of the proposed metamaterial cell, and (c) the simulated phase of S11 of the metamaterial with different a1.

To further enhance the gain, a four-element microstrip MIMO antenna array with a cover layer consists of the MSS is proposed and is shown in Fig. 3 (a). The metamaterial is comprised of only one layer, which has 13 by 9 MSS cells, and it is illustrated in Fig. 3 (a). In this design, the metamaterial is printed on the FR4 substrate. The cover layer is fixed above the antenna array by using four plastic bolts at each corner. The distance from patch antenna array to the bottom surface of the cover layer is h2=30mm, which is large enough so that the near-field interaction is not obvious between the radiation of the antenna array and MSS. Therefore, the performance of the MIMO antenna array is basically unaffected by the cover layer that is comprised of MSS cells. The finalized model of the four-element MIMO antenna array with metamaterial cover layer is shown in Fig. 3 (b), and its physical dimensions are listed in Table 1. Since a portion of the electromagnetic waves radiate into space from the MSS, the remaining energy is reflected to the other antenna elements owing to the loading, which results in a space mutual coupling between transmitting antenna and receiving antenna.

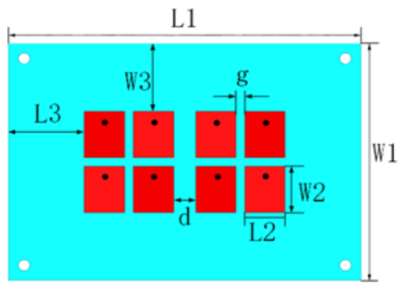

(a)

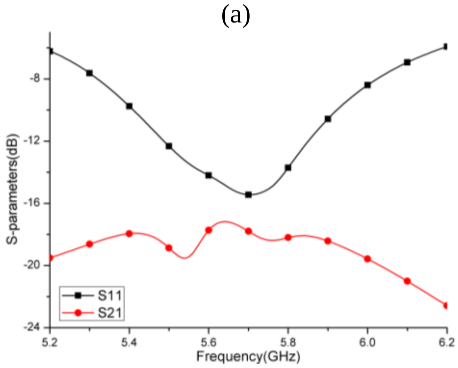

(b)

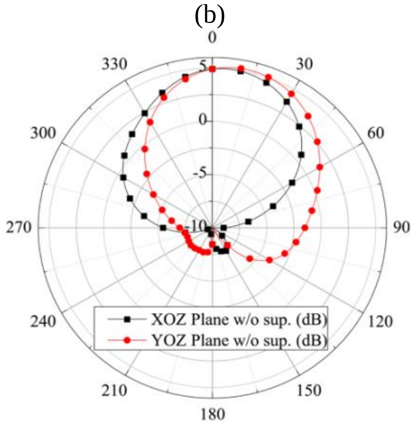

(c)

Fig. 2. (a) The configuration of the original four-element MIMO antenna, (b) simulated S-parameters, and (c) simulated radiation pattern.

C. High isolation antenna array with gain enhancement

In this paper, the gain of the proposed MIMO antenna array is enhanced by using loaded MSS, which might give some effects on its mutual coupling. To reduce the mutual decoupling in the designed MIMO antenna array, a mutual coupling network is utilized to implement the isolation enhancement. Fig. 4 (a) gives schematic of MIMO antenna array with the proposed mutual decoupling network. Figure 4 (b) shows the structure of the designed mutual decoupling network. From Fig. 4 (b), it is found that the mutual decoupling network is composed of two stage transmission line with electric length of θ, characteristic impendence of Z_0, and a parallel reactance component with a value of jB. The decoupling mechanism is concluded as follows. By connecting the transmission lines with parallel reactance component, a partial input signal from Port 1 can be indirectly coupled to Port 2, which is named as indirect coupling hereafter. The magnitude of the indirect coupling can be controlled to reduce the mutual coupling caused by space waves and surface waves.

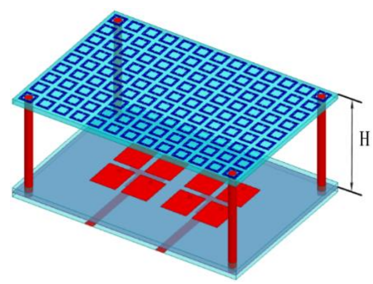

(a)

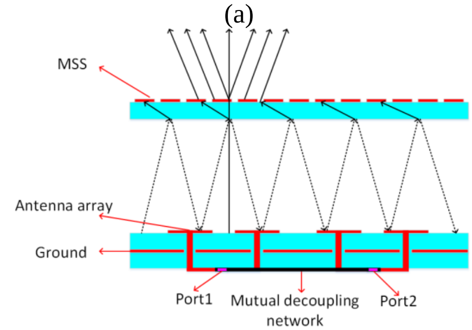

(b)

Fig. 3. (a) The configurable of the proposed four-element MIMO antenna with MSS loading, and (b) radiation model of the proposed four-element MIMO antenna with MSS loading.

Table 1: Parameters of the MIMO antenna array with metamaterial coating

Parameter	L1	L2	L3	g1	W1	W2	W3	A
Value (mm)	79	9	17	0.3	55	10.7	15.8	6
Parameter	g2	t	d	g	H	h1	c	a1
Value (mm)	0.3	0.2	5	2	34.8	1.6	0.3	4.55

Next, to better understand the effects of parameters θ, Z_0, jB , and to optimize the performance of the design, parameters studies are carried out to give a good performance by totally considering the MIMO antenna array and mutual decoupling network. A symmetrical antenna array without decoupling network is characterized by a scattering matrix $[S^A]$, which can be expressed as:

$$\left[S^A\right]=\begin{bmatrix} 0 & \alpha e^{j\varphi} \\ \alpha e^{j\varphi} & 0 \end{bmatrix}. \tag{2}$$

The parameters α and φ are the amplitude and phase of the mutual coupling between the MIMO antenna array, respectively. We utilize the transmission lines with a characteristic impedance of Z_0 at the two ports of the MIMO antenna array, resulting in a phase delay of 2θ to the coupling coefficient. Therefore, the modified scattering matrix $[S^{A^1}]$ can be obtained, and it can be transformed into an admittance matrix of $[Y^{A^1}]$. In this paper, the matrix of $[S^{A^1}]$ is expressed as:

$$\left[S^{A^1}\right]=\begin{bmatrix} 0 & \alpha e^{j(\varphi-2\theta)} \\ \alpha e^{j(\varphi-2\theta)} & 0 \end{bmatrix}. \tag{3}$$

The transmission lines not only act as delay lines between the MIMO antenna array elements and parallel reactance component, but also it can transform the complex admittance matrix of the mutual coupling into a pure imaginary admittance matrix that can be canceled by the parallel reactance component. $[Y^b]$ is the scattering parameter of the two-port network consisting of the parallel reactive components, which can be expressed as:

$$\left[Y^b\right]=\begin{bmatrix} jB & -jB \\ -jB & jB \end{bmatrix}. \tag{4}$$

Thus, the admittance matrix after adding the parallel reactance component is:

$$\left[Y^B\right]=\left[Y^{A^1}\right]+\left[Y^b\right], \tag{5}$$

$$Y_{21}^B=Y_{12}^B=Y_0\left(\frac{-2\alpha e^{j(\varphi-2\theta)}}{1-\alpha^2 e^{j2(\varphi-2\theta)}}\right)-jB, \tag{6}$$

$$Y_{11}^B=Y_{22}^B=Y_0\left(\frac{1+\alpha^2 e^{j2(\varphi-2\theta)}}{1-\alpha^2 e^{j2(\varphi-2\theta)}}\right)+jB, \tag{7}$$

$$Y=\frac{1}{Z_0}. \tag{8}$$

According to the conversion relationship between Y-parameter and S-parameter, the S-parameter after adding the parallel reactance element can be obtained:

$$S_{21}^B=\frac{-Y_{21}^B Y_0}{Y_0^2+2Y_{11}^B+(Y_{11}^B)^2-(Y_{21}^B)^2}, \tag{9}$$

$$S_{11}^B=\frac{Y_0^2-2Y_{11}^B-(Y_{21}^B)^2}{Y_0^2+2Y_{11}^B+(Y_{11}^B)^2-(Y_{21}^B)^2}. \tag{10}$$

To obtain the isolation enhancement after loading the mutual decoupling network, the parameter of S_{21}^B must be 0, which means that the Y_{21}^B should be set as 0. Hence, a relationship can be obtained as follows:

$$\theta=\frac{1}{2}\left(\varphi\pm\frac{\pi}{2}\right), \tag{11}$$

$$B=\pm\frac{2\alpha}{1+\alpha^2}Y_0. \tag{12}$$

In addition, the L-shaped branch is utilized to get a better match. The length and the width of the parallel reactance component that gives important effects on the mutual decoupling network are investigated in detail. Figure 5 (a) gives the S-parameter of the MIMO antenna array after adding the mutual decoupling with different length *L* ranging from 16mm to 20mm.

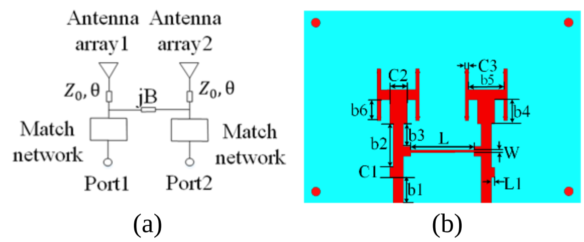

Fig. 4. (a) The schematic of the proposed mutual decoupling network in the MIMO antenna array, and (b) the mutual decoupling network.

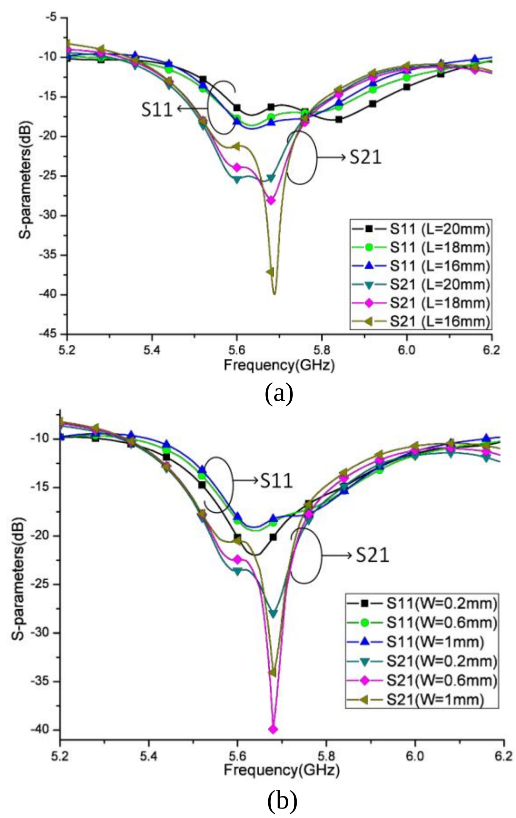

Fig. 5. (a) S-parameters of the MIMO antenna array with different *L*. (b) S-parameters of the MIMO antenna array with different *W*.

Figure 5 (b) shows the S-parameter of the MIMO antenna array after adding the mutual decoupling with different width *W* ranging from 0.2mm to 1mm. The isolation between antenna array elements becomes higher with an increasing *L*. And, it also can be seen that when W is 0.6mm, a higher isolation can be gotten. If W is getting larger than the *0.6mm*, the isolation becomes worse. Then, the length of the L-shaped branch increasing from 1mm to 3mm is investigated to reach a good match. Figure 6 illustrates the effect with different length L1 on the S-parameter of the MIMO antenna array.

The center frequency of the S11 moves to higher frequency with an increasing of L1. The optimized parameters for the mutual decoupling network of the MIMO antenna array are listed in Table 2.

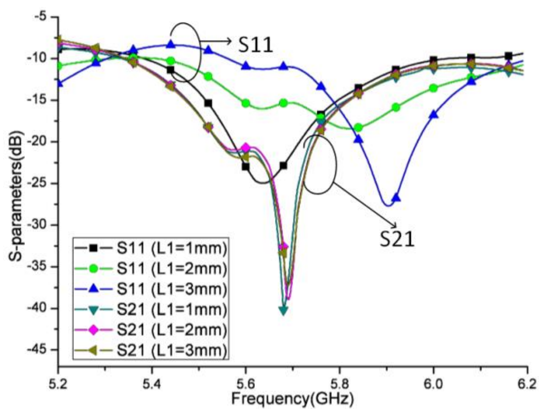

Fig. 6. S-parameters of the MIMO antenna array with different L1.

Table 2: The optimized parameters of the mutual decoupling network of the MIMO antenna array

Parameters	b1	b2	b3	b4	b5	b6
Value (mm)	7.5	12.39	6.39	6.82	10	5.92
Parameter	C1	C2	C3	L	W	L1
Value (mm)	2.86	4.87	1	18	0.63	1

III. PERFORMANCE OF THE PROPOSED MIMO ANTENNA ARRAY

In this paper, a high isolation MIMO antenna array with metamaterial loading and mutual decoupling network and gain enhancement is proposed and analyzed by using the HFSS. Herein, a mutual decoupling network is utilized to cancel the surface waves and space waves between antenna array elements since the metamaterial loading might also give some interferences from the adjacent antenna elements. The designed high isolation MIMO antenna array with gain enhancement is optimized, fabricated and measured. The photograph of the fabricated MIMO array is shown in Fig. 7. The S-parameter, radiation patterns, surface current distribution, and vector magnetic, and electric fields in the XOZ-plane are presented when one antenna array is excited while another antenna array is terminated by 50-Ohm.

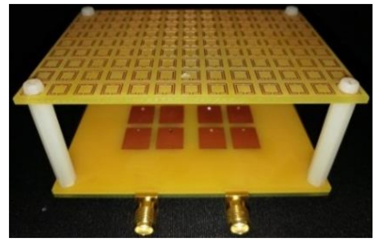

Fig. 7. The photograph of the fabricated MIMO antenna array.

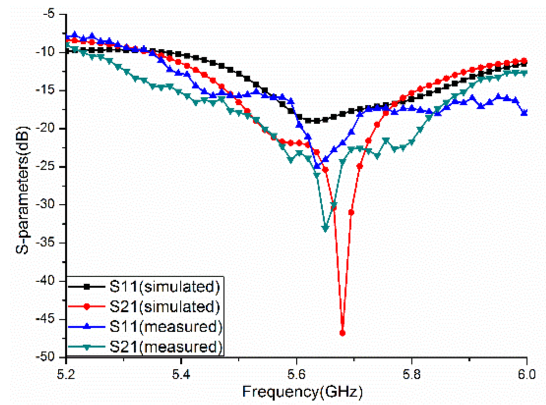

Fig. 8. S-Parameters of the proposed MIMO antenna array.

First, the S-parameters of the fabricated MIMO antenna array with loading MSS and mutual decoupling network are shown in Fig. 8. It can be seen that the proposed MIMO antenna array operates at 5.42-5.95 GHz covering the 5.8GHz WLAN band. The isolation of the MIMO antenna array is improved by about 30dB by using the proposed decoupling network and the MSS loading. Then the radiation patterns of the MIMO antenna array are measured in a chamber with NSI measurement system, which are shown in Fig. 9. From Fig. 2 (a), we can see that the peak gain of the developed MIMO antenna array without the MSS loading and the neutralization line structure is 5.3dB. By using the MSS and the neutralization line structure, our developed MIMO antenna array has a gain of 8.3 dB, which is shown in Fig. 9 (a). Thus, the proposed techniques can achieve a gain enhancement of 3dB.

To explain the mechanism of the mutual decoupling and gain enhancement for the space waves, the simulated vector magnetic field distribution and electric field contours are investigated and presented in Fig. 10. Without the mutual decoupling structure, the magnetic-field vector along the substrate of the MIMO antenna array propagates to the right direction while the magnetic-field vector returned to the left direction of by using the decoupling network, which can reduce the mutual coupling. The electric field of the MIMO antenna array without and with the designed mutual decoupling are shown in Figs. 10 (c) and (d) respectively. The left antenna array is excited, while the right antenna array is induction antenna array. It can be seen that large electric field energy is radiated to the space without mutual decoupling, while the electric field energy is concentrated on the normal direction of the antenna array with the help of the MSS loading. Compared with the electric field distribution, there are more energy is radiated in the target direction, which means that less energy is radiated to the right antenna array. Therefore, after loading the MSS, the mutual decoupling, a high isolation and gain enhancement can be obtained. The radiation efficiency of the designed high gain and isolation antenna array is 68%.

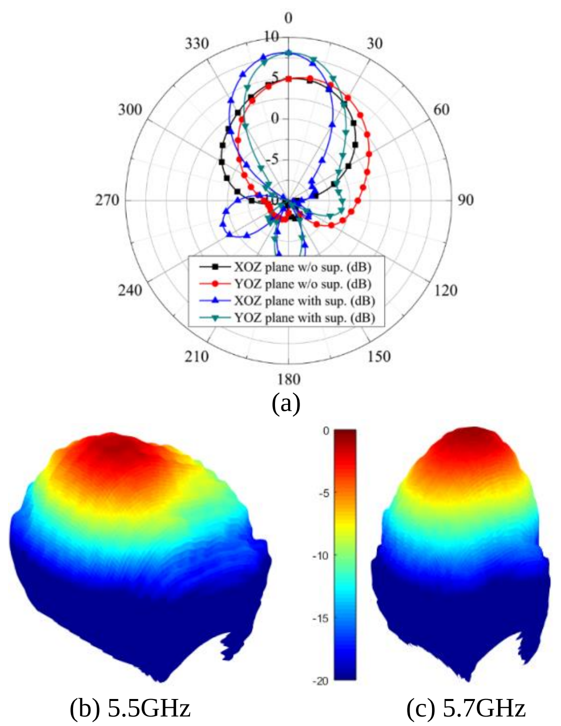

Fig. 9. (a) Simulated radiation patterns of the proposed antenna array with and without MSS loading. (b), (c) Measured radiation patterns of the proposed MIMO antenna array (unit: dB).

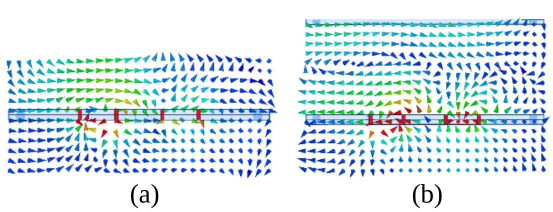

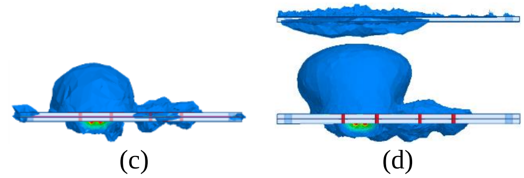

Fig. 10. (a) Simulated vector magnetic field distribution without mutual decoupling structure. (b) Simulated vector magnetic field distribution with mutual decoupling structure. (c) Simulated electric field contours without mutual decoupling structure. (d) Simulated electric field contours with mutual decoupling structure.

VI. CONCLUSION

In this paper, a high gain and high isolation MIMO antenna array has been proposed by using MSS loading and mutual decoupling structure, and its performance is analyzed and optimized by the use of both the simulations and measurements. The MSS loading consists of 13×9 metamaterial cells that are set above the MIMO antenna array to enhance the gain of the proposed antenna. The proposed antenna array has a gain and isolation enhancement about 3dB and 30dB, respectively, over the operating band within the upper WLAN communication band. The design of the MIMO antenna array with high performance has a great application prospect in based stations for WLAN communications.

ACKNOWLEDGMENT

This work was partially supported by the National Key Research and Development Program of China (2016YFE111100), Key Research and Development Program of Heilongjiang (GX17A016), the Science and Technology innovative Talents Foundation of Harbin (2016RAXXJ044), the Natural Science Foundation of Beijing (4182077), China Postdoctoral Science Foundation (2017M620918) and the Fundamental Research Funds for the Central University (HEUCFM180806).

REFERENCES

[1] Y. Li, W. Li, and W. Yu, “A multi-band/UWB MIMO/diversity antenna with an enhance isolation using radial stub loaded resonator,” *Applied Computational Electromagnetics Society Journal*, vol. 28, no. 1, pp. 8-20, 2013.

[2] Z. Wang, G. Zhang, and Y. Yin, “Design of a dual-band high-gain antenna array for WLAN and WiMAX base station,” *IEEE Antennas and Wireless Propag. Lett.*, vol. 13, pp. 1721-1724, 2014.

[3] Y. Li, W. Li, and W. Yu, “A switchable UWB slot antenna using SIS-HSIR and SIS-SIR for multi-mode wireless communications applications,” *Applied Computational Electromagnetics Society Journal*, vol. 27, no. 4, pp. 340-351, 2012.

[4] R. A. Alhalabi and G. M. Rebeiz, "High-gain Yagi-Uda antennas for millimeter-wave switched-beam syatem," *IEEE Trans. Antennas Propag*., vol. 57, no. 11, pp. 3672-3676, 2009.

[5] W. Yang, J. Zhou, Z. Yu, and L. Li, "Bandwidth and gain-enhanced circularly polarized antenna array using sequential phase feed," *IEEE Antennas Wireless Propag. Lett*., vol. 13, pp. 1215-1218, 2014.

[6] A. E. I. Lamminen, J. Saily, and A. R. Vimpari, "60-GHz patch antennas and arrays on LTCC with embedded-cavity substrates," *IEEE Trans. Antennas Propag*., vol. 56, no. 9, pp. 2865-2874, Sep. 2008.

[7] S. Yeap, Z. Chen, and X. Qing, "Gain-enhanced 60-GHz LTCC antenna array with openair cavities," *IEEE Trans. Antennas Propag*., vol. 59, no. 9, pp. 3470-3473, 2011.

[8] B. Cao, H. Wang, Y. Huang, and J. Zheng, "High-gain L-probe excited substrate integrated cavity antenna array with LTCC-based gap waveguide feeding network for W-band application," *IEEE Trans. Antennas Propag*., vol. 63, no. 12, pp. 5465-5474, 2015.

[9] J. Liu, Z. Tang, Z. Wang, et al., "Gain enhancement of a broadband symmetrical dual-loop antenna using shorting pins," *IEEE Antennas Wireless Propag. Let*., vol. 17, no. 8, pp. 1369-1372, 2018.

[10] A. E. I. Lamminen, A. R. Vimpari, and J. Saily, "UC-EBG on LTCC for 60-GHz frequency band antenna applications," *IEEE Trans. Antennas Propag*., vol. 57, no. 10, pp. 2904-2912, 2009.

[11] H. Zhou, Z. Pei, and S. Qu, "A novel high-directivity microstrip patch antenna based on zero-index metamaterial," *IEEE Antennas Wireless Propag. Let*., vol. 8, pp. 538-541, 2009.

[12] D. Ramaccia, F. Scattone, F. Bilotti, et al., "Broad-band compact horn antennas by using EPS-ENZ metamaterial lens," *IEEE Trans. Antennas Propag*., vol. 61, no. 6, pp. 2929-2937, 2013.

[13] Y. Li, Z. Zhang, J. Zheng, and Z. Feng, "Compact azimuthal omnidirectional dual-polarized antenna using highly isolated co-located slots," *IEEE Trans. Antennas Propag*., vol. 60, no. 9, pp. 4037-4045, 2012.

[14] Y. Li, Z. Zhang, Z. Feng, and M. F. Iskander, "Design of omnidirectional dual-polarized antenna in slender and low-profile column," *IEEE Trans. Antennas Propag*., vol. 62, no. 4, pp. 2323-2326, 2014.

[15] Y. Li, W. Li, and Q. Ye, "A reconfigurable triple notch band antenna integrated with defected micro-strip structure band-stop filter for ultra-wideband cognitive radio applications," *International Journal of Antennas and Propagation*, vol. 2013, Article ID: 472645, pp. 1-13, 2013.

[16] K. Wei, J. Li, L. Wang, Z. Xing, and R. Xu, "S-shaped periodic defected ground structures to reduce microstrip antenna array mutual coupling," *Electronics Letters*, vol. 52, pp. 1288-1290, 2016.

[17] K. Wei, J. Li, L. Wang, Z. Xing, and R. Xu, "Mutual coupling reduction by novel fractal defected ground structure bandgap filter," *IEEE Trans. Antennas Propag*., vol. 64, pp. 4328-4335, 2016.

[18] F. Yang and Y. Rahmat-Samii, "Microstrip antennas integrated with electromagnetic band-gap (EBG) structures: A low mutual coupling design for array applications," *IEEE Trans. Antennas Propag*., vol. 51, no. 10, pp. 2936-2946, 2003.

[19] T. Jiang, T. Jiao, and Y. Li, "Array mutual coupling reduction using L-loading E-shaped electromagnetic band gap structures," *International Journal of Antennas and Propagation*, vol. 2016, Article ID 6731014, 9 pages, 2016.

[20] T. Jiang, T. Jiao, and Y. Li, "A low mutual coupling MIMO antenna using periodic multi-layered electromagnetic band gap structures," *Applied Computational Electromagnetics Society Journal*, vol. 33, no. 3, 2018.

[21] M. A. Abdalla and A. A. Ibrahim, "Compact and closely spaced metamaterial MIMO antenna with high isolation for wireless applications," *IEEE Trans. Antennas Propag*., vol. 12, pp. 1452-1455, 2013.

[22] K. Yu, Y. Li, and X. Liu, "Mutual coupling reduction of a MIMO antenna array using 3-D novel meta-material structures," *Applied Computational Electromagnetic Society Journal*, vol. 33, no. 7, pp. 758-763, 2018.

[23] D. A. Ketzaki and T. V. Yioultsis, "Metamaterial-based design of planar compact MIMO monopoles," *IEEE Trans. Antennas Propag*., vol. 61, no. 5, pp. 2758-2766, 2013.

[24] L. Zhao, F. Liu, X. Shen, G. Jing, Y. Cai, and Y. Li, "A high-pass antenna interference cancellation chip for mutual coupling reduction of antennas in contiguous frequency bands," *IEEE Access*, vol. 6, pp. 38097-38105, 2018.

[25] R. Xia, S. Qu, P. Li, D. Yang, S. Yang, and Z. Nie, "Wide-angle scanning phased array using an efficient decoupling network," *IEEE Trans. Antennas Propag*., vol. 63, no. 11, 2015.